68Ga-NOTA-UBI-29-41 as a PET Tracer for Detection of Bacterial Infection

Mónica Vilche, Ana Laura Reyes, Elena Vasilskis, Patricia Oliver, Henia Balter*, and Henry Engler*

Uruguayan Centre of Molecular Imaging, Montevideo, Uruguay

The cationic peptide 68Ga-NOTA-UBI-29-41 was synthesized and characterized. Biodistribution and PET/CT examinations were performed for evaluation of its biologic behavior. Differentiation of infection from sterile inflammation was investigated using microbiology methods at the sites of bacterial infections. **Methods:** Labeling of UBI-29-41 conjugated with NOTA with 68Ga was optimized at 20°C–100°C and pH 3.5–5.5. Radiochemical purity, stability up to 260 min, and binding to serum proteins were determined. In vitro binding to *Staphylococcus aureus* was evaluated from 9.14×10^7 to 1.17×10^{10} cfu/mL. Of 3 groups of *Mus musculus* Swiss male mice, the first was inoculated intramuscularly with 1.2×10^8 cfu of *S. aureus* to provoke infection, and the second, with 1.2×10^8 cfu of heat shock–treated *S. aureus* to generate sterile inflammation. The third mouse was not treated and served as a control. After 24 h, 68Ga-NOTA-UBI-29-41 was administrated intravenously, and biodistribution was performed at 30, 60, and 120 min. PET/CT dynamic studies (120 min) were acquired. Sinograms were reconstructed using 3D maximum-likelihood expectation maximization and analyzed with software. Infected or inflamed muscles were dissected, homogenized, and cultured in tryptic soy agar medium. Recovered *S. aureus* was calculated as cfu/g. **Results:** 68Ga-NOTA-UBI-29-41 showed high renal excretion (83.2% ± 7.3%) of injected dose and rapid blood clearance. More than 95% was bound in vitro to 5×10^9 cfu/mL. A significantly higher ($P < 0.05$) accumulation of 68Ga-NOTA-UBI-29-41 was observed at sites of *S. aureus* inoculation in infected mice (ratio of target to nontarget, 5.0 at 60 min and 4.1 at 120 min) compared with animals with inflammation (ratio of target to nontarget, 1.6 at 60 min and 1.2 at 120 min). **Conclusion:** The difference in uptake of 68Ga-NOTA-UBI-29-41 in the infected muscles compared with the inflamed muscles was clearly observed in the PET/CT images and positively correlated with the degree of infection.

Key Words: ubiquicidin-derived peptide; UBI-29-41; 68Ga; infection diagnosis; PET/CT

T he differential diagnosis between bacterial infection and sterile inflammation is important. The development of new molecules labeled with positron emitters can improve the sensitivity and specificity of the diagnosis (*1*). During the past decade, many efforts have been devoted to the development of new radiopharmaceuticals for detecting infection. A gradual shift occurred from large proteins with a nonspecific uptake mechanism to more specific targeting. Today, neutrophil-mediated processes, which are characteristic of both inflammatory and infectious processes, can be targeted in situ by radiolabeled leukocytes, antibodies or their fragments, cytokines, and 18F-FDG. A newer promising alternative is the direct targeting of viable bacteria or fungi with radiolabeled antimicrobial compounds (*2*). Recently, a synthetic compound derived from the human antimicrobial peptide ubiquicidin (UBI) labeled with 99mTc has been used to distinguish bacterial infections from sterile inflammatory processes and to monitor the efficacy of antibiotic therapy (*3–5*). UBI derivatives—human antimicrobial peptides present in epithelial cells of the respiratory system of mammalians—are some of the most promising diagnostic markers. They act as a first line of defense against infiltrating pathogens (*6*). Welling et al. (*3*) investigated several of these peptides and concluded that the UBI cationic peptide 29-41 (molecular weight, 1,693 Da, with the amino acid sequence Thr-Gly-Arg-Ala-Lys-Arg-Arg-Met-Gln-Tyr-Asn-Arg-Arg), derived from the bacterial binding domain of this antimicrobial peptide, is an optimal candidate for the differentiation of infection from inflammation. 99mTc-UBI-29-41 has been tested for specific imaging of bacterial and fungal infections in mice, rats, and rabbits, and for monitoring a decrease in viable pathogens after antimicrobial therapy (*5*). 99mTc-UBI-29-41 has a high potential for specific imaging of infections. Sterile inflammation and tumors are not detected, allowing the differential diagnosis (*7*). The labeling of UBI-29-41 with 68Ga is of special interest for use as a PET tracer. This radiopharmaceutical is nontoxic and has a half-life of 68 min, making it suitable for peptide pharmacology. 68Ga is available from 68Ge/68Ga generators without using a cyclotron (*8*). The introduction of bifunctional macrocyclic complexing agents has led to agents with slower rates of decomposition (*9,10*). Ligands such as NOTA and DOTA have been used in conjunction (complexation) with 111In and 67Ga or 68Ga (*11*). DOTA and NOTA can be attached to a carrier molecule via the carboxylate group or the functionalized carbon skeleton. This method allows a one-step coupling reaction to amines using carbodiimide chemistry (*12*). The neutral Ga(III) complex of NOTA has been shown to undergo acid-catalyzed dissociation only at low pH levels, which is unlikely in physiologic conditions. The 68Ga-NOTA complex has high thermodynamic and kinetic stability (*13*). The aim of this study was to optimize parameters such as pH, buffer systems, and time of incubation that affect the labeling of 68Ga-NOTA-UBI-29-41 and its quality control. In vitro studies were performed using the radiolabeled peptide with increasing amounts of *S. aureus*. In vivo studies included the evaluation of the tracer in mouse models developed to express infection or sterile inflammation (*14*).

MATERIALS AND METHODS

Synthesis of ^{68}Ga-NOTA-UBI-29-41

The 29-41 amino acid fragment of ubiquicidin (UBI-29-41) conjugated with NOTA (NOTA-UBI-29-41, molecular weight, 1978.25; purity > 90%; piCHEM) was used for ^{68}Ga labeling. ^{68}Ga was obtained as GaCl$_3$ or, alternatively, from a generator (IGG100; Eckert & Ziegler or Isotope Technologies Garching) by fractionated elution with HCl (31.5% by acidimetry, Suprapure; Merck) of 0.1 or 0.05 M, respectively, to get the highest activity concentration. Activity levels in 1.2- to 2.5-mL fractions ranged from 200 to 650 MBq. For the optimization of labeling parameters, 5–60 nmol of NOTA-UBI-29-41(1 mM) in ultrapurified water were mixed with 1.5–80 μL of sodium acetate buffer, 5 M, pH 4.6 (prepared with sodium acetate, 100.00% Suprapure; and acetic acid ≥ 99.9% by acidimetry, Suprapure). Six to 160 MBq of ^{68}GaCl$_3$ were added. For mouse experiments, 30 nmol of NOTA-UBI-29-41 and approximately 30 MBq of ^{68}Ga were used. pH was determined before incubation at 20°C, 90°C, and 100°C. The effect of pH in labeling yield was evaluated for pH 3.5–5.5. The minimum amount of buffer to reach the desired pH was determined and used for minimizing the ionic strength. All the reagents were selected to minimize the presence of metal contaminants such as iron and others.

Radiochemical Purity of ^{68}Ga-NOTA-UBI-29-41. Radiochemical purity was monitored by high-performance liquid chromatography (HPLC) on C-18 columns (4.6 × 150 mm, 5 μm) (ZORBAX Eclipse Plus C18; Agilent) with gradient 0.1% trifluoroacetic acid in H$_2$O and 0.1% trifluoroacetic acid in acetonitrile, from 100% to 40% in 6 min and 40% until 10 min with a flow of 1 mL/min. Instant thin-layer chromatography on silica gel (ITLC-SG; Varian) was run in citric acid 0.1 M and measured on EZ-SCAN (Carroll and Ramsey Associates) using PeakSimple chromatography software (SRI Instruments). The R$_f$ of ^{68}Ga-NOTA-UBI-29-41 was 0.0, whereas for ^{68}GaCl$_3$, it was 0.75–0.85. Purification was done on solid-phase extraction (SPE) using Sep-Pak C18 Light (Waters) previously activated with 5 mL each of ethanol and water. Seven microliters of the reaction mixture were applied. Hydrophilic impurities (^{68}GaCl$_3$) were eluted with 5 mL of acetic acid, 0.1%, and the labeled peptide was eluted with 1 mL of ethanol, 50%, and washed with 8 mL of saline. ^{68}Ga colloid remained in the cartridge. Samples and cartridge were measured in a 7.62 × 7.62 cm (3 in × 3 in) NaI(Tl) γ-counter (Ortec).

Specific Activity. Specific activity was determined by the ratio between activity and peptide amount, quantified by ultraviolet interpolation in a standard curve with a lower detection limit of 5 × 10^{-7} M, equivalent to 5 pmol in the sample. For this calculation, the data were obtained from HPLC.

Stability. Stability was monitored up to 260 min by HPLC and ITLC-SG.

Binding of ^{68}Ga-NOTA-UBI29-41 to Proteins

Binding of ^{68}Ga-NOTA-UBI29-41 to proteins was determined by molecular exclusion using permeation columns (Illustra MicroSpin G-50; GE Healthcare). Seventy microliters of ^{68}Ga-NOTA-UBI-29-41 were incubated with 700 μL of human serum in a 1:10 dilution at 37°C and for different times: 30, 60, 90, and 120 min. Phosphate-buffered saline was used as a control.

Biologic Evaluation

The in vitro binding of ^{68}Ga-NOTA-UBI-29-41 to *S. aureus* was assessed as previously described (*4*) by incubation for 1 h at 4°C. Electrostatic interactions between the cationic peptides and the negatively charged residues in the bacterial membrane contributed to the binding peptide-bacteria depending on the pH and the high salt concentrations. For preparation of *S. aureus* samples (25923; ATCC), 1.2 × 10^{10} cfu in 0.4 mL of phosphate buffer, 14 mM, pH 7.5, were

serially diluted 1:2 in saline 7 times in duplicate Eppendorf-type vials. Final vials contain from 1.17 × 10^9 to 9.14 × 10^6 cfu in 0.1 mL. To each of those, 0.8 mL of 50% (v/v) 0.01 M acetic acid in phosphate buffer supplemented with 0.01% (v/v) polysorbate-80 was added. After this step, 0.1 mL of a 1:10 dilution of the ^{68}Ga-labeling solution in phosphate buffer, 14 mM, pH 7.5, containing 2.4 nmol of peptide and 1.7 MBq was transferred to the vials containing the *S. aureus* dilutions. The mixture was incubated for 1 h at 4°C and centrifuged at 2,500*g* for 5 min at 4°C. Total activity was measured in a 7.62 × 7.62 cm (3 in × 3 in) well scintillation counter. The supernatant was removed, and the pellet was gently resuspended in 1.0 mL of phosphate buffer supplemented with 0.01% (v/v) polysorbate-80 and recentrifuged as explained previously. Radioactivity in the pellet was determined. The radioactivity bound to bacteria and was expressed as a percentage of the total added ^{68}Ga activity.

Animal Studies. Studies were performed according to national and international guidelines for the use of animals for research. The Bioethics Committee of the Uruguayan Centre of Molecular Imaging approved this study.

Preparation of Animal Models. Three groups of *M. musculus* Swiss male mice, 25–30 g, aged 11–12 wk, were used. In the first group, infection was induced by inoculation of 0.1 mL of *S. aureus* (1.2 × 10^9 cfu/mL) in the left upper thigh muscle. In the second group, inflammation was induced by inoculation of 0.1 mL of heat shock–treated *S. aureus* (1.2 × 10^9 cfu/mL) in the same region. The third group consisted of healthy mice.

Ex Vivo Studies. Biodistribution studies were performed 24 h after inoculation. Four animals per group were injected with 2.6 ± 0.5 MBq, 4.2 ± 1.3 MBq, and 7.5 ± 1.9 MBq (50–150 μL) of ^{68}Ga-NOTA-UBI-29-41 in the caudal tail vein and were sacrificed by cervical dislocation at 30, 60, and 120 min after injection. Another group was injected with the radiopharmaceutical 48 h after inoculation with *S. aureus*. In these mice, biodistribution was studied at 1 h (*n* = 2) and 2 h (*n* = 1) after inoculation. All organs, samples of blood, and the thigh muscles (left as target, right as control) were dissected, weighed, and assayed for radioactivity. Total urine volume was collected during the biodistribution period or removed from the bladder after sacrifice, and its activity was measured. The percentage injected dose per gram of tissue and injected dose in the whole organ were calculated, as well as the target-to-nontarget (T/NT) ratio of muscles.

Image Acquisition. PET/CT imaging in mice was performed using a trimodality scanner (Triumph; Gamma Medica, Inc.) with lutetium yttrium oxyorthosilicate and lutetium gadolinium oxyorthosilicate scintillators (LabPET) (spatial resolution, 1.0 mm; axial field of view, 3.75 cm). Data were acquired in list mode in a 184 × 184 × 31 matrix with a pixel size of 0.25 × 0.25 × 1.175 mm and a coincidence window width of 22.22 ns. The animals were anesthetized with 2% isoflurane in an oxygen flow of 2 L/min, placed prone on the scanner bed, and intravenously injected with 50–150 μL of ^{68}Ga-NOTA-UBI-29-41 (7.5 ± 1.9 MBq). Dynamic studies were performed for all groups during 120 min (4 frames × 30 min and 24 frames × 5 min). Sinograms were reconstructed using 3D maximum-likelihood expectation maximization.

Image Analysis. Semiquantitative analysis was done using PMOD software, version 3.4. PET studies were coregistered with the corresponding CT studies for anatomic localization. Volumes of interest were drawn on 2 selected thigh muscle regions (left as target, right as control or nontarget) to analyze their specific uptake. SUVs normalized for injected dose and body weight were calculated and averaged for each group.

Confirmation of Infection. The dissection of infected muscle in aseptic conditions and its homogenization and culture were performed to confirm the presence of infection and to correlate the specific uptake of ^{68}Ga-NOTA-UBI-29-41 with the colony-forming units of

S. aureus per gram of muscle (*3*). The dissected target and nontarget muscles were homogenized (T-25 digital ULTRA-TURRAX; IKA-Werke GmbH & Co.) in 5.0 mL of phosphate-buffered sulfate, 0.015 M, pH 7.2, and diluted 1:10 from 10^{-1} to 10^{-4}. One milliliter of each dilution was plated on trypticase soy agar and incubated for 24–48 h. The number of colony-forming units was determined, and results were expressed as cfu/g of tissue. The same procedure was performed for the contralateral muscle of infected muscles and for inflamed muscles.

RESULTS

Synthesis and Radiolabeling of ^{68}Ga-NOTA-UBI-29-41

Optimization of Labeling Parameters. For pH evaluation, we used the range recommended (3.5–4.5) in the bibliography (*1,8, 12,13,15*), in which the effect of pH in the labeling with ^{68}Ga is thoroughly analyzed. We also tested several buffer pH settings and concentrations to achieve robust conditions for the labeling, reaching optimal conditions for pH in the recommended range and minimizing salt concentration. The effect of temperature is shown in Table 1. High yields were obtained for both temperatures; but at 90°C the reaction labeling proceeded faster, requiring only 5 min to reach more than 95%.

Radiochemical Purity. As to whether 96% ± 3% ($n = 16$) was in the optimized conditions—90°C for 5 min and pH 3.5–4.0—Figure 1 shows a typical HPLC profile. Retention times for labeled and unlabeled UBI-29-41 were 6.825 ± 0.024 min and 6.746 ± 0.029 min, respectively. ^{68}Ga colloid determination by Sep-Pak C18 correlated well with the HPLC and ITLC-SG results. The amount of colloid was 1.1% ± 1.3%. Labeling yield evaluated for different peptide-to-activity ratios is shown in Figure 2. Maximum yield and radiochemical purity were reached for 30 nmol of NOTA-UBI-29-41 and 30 MBq incubating at 20°C for 10 min. Specific activity calculated from the HPLC ultraviolet calibration curve was 0.55 MBq/nmol.

Stability of ^{68}Ga-NOTA-UBI-29-41. The stability of the peptide was confirmed up to 3 h, showing no decrease from the initial 97% value during this time.

Binding of ^{68}Ga-NOTA-UBI-29-41 to Proteins. The binding of ^{68}Ga-NOTA-UBI-29-41 ranged from 37% to 52% during the time studied (30–120 min), as shown in Table 2.
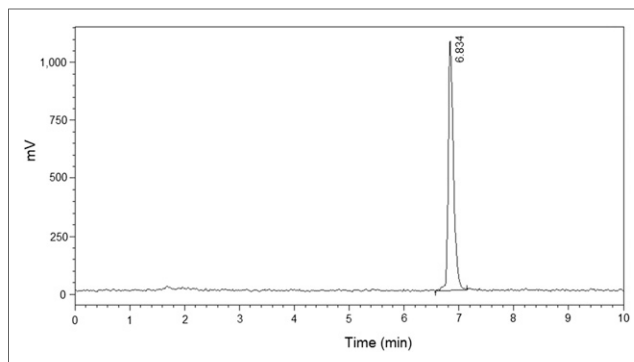
Biologic Evaluation

In Vitro Binding of ^{68}Ga-NOTA-UBI-29-41 to S. Aureus. We found a logarithmic increase dependent on the number of bacteria and reaching 95% ± 11% for 5×10^8 cfu, with a maximum of 97% ± 2% for 1.17×10^9 cfu (Fig. 3). Binding to bacteria is evident even for low amounts of *S. aureus* (19.2% of the total activity for 9.14×10^6 cfu).

FIGURE 1. HPLC profile of ^{68}Ga-NOTA-UBI-29-41.

Biodistribution of ^{68}Ga-NOTA-UBI-29-41. High renal excretion and rapid blood clearance were observed in all groups (Fig. 4). In healthy mice, activity eliminated by urine reached 83.2% ± 7.3% injected dose in 2 h. Swelling, increased vascularization, and pus were observed in the infected thigh muscle, but no pus was seen in the inflamed muscles. Even large lymph nodes were observed in infected mice. Microbiologic assays determined that the changes were related to bacterial growth. The ratio of infected muscle (activity/gram) or inflamed muscle compared with the healthy leg (T/NT) reached 5.0 at 60 min and 4.1 at 120 min. For the mice with inflamed muscles, these values were 1.6 and 1.2, respectively (Fig. 5). When the inoculation of *S. aureus* was done 48 h before the administration of ^{68}Ga-NOTA-UBI-29-41, the T/NT ratio reached 4.16 ± 0.02 ($n = 2$) 1 h after injection and 9.4 ($n = 1$) at 2 h. ANOVA and Tukey statistical testing showed a *P* value of 0.002 or less for the T/NT of the group of infected mice compared with the groups of inflamed and healthy mice for all the times studied. No significant differences ($P = 0.817$) were found among the groups of healthy and inflamed mice, demonstrating the ability to distinguish infection from inflammation.

PET/CT Imaging. T/NT ratios calculated from PET/CT images for infected mice were greater than 2.4 at 10 min, increased gradually to a maximum of more than 4.0 at 60 min, and decreased slightly after 80 min (T/NT > 3.4) after injection (Fig. 5B). All

TABLE 1
Labeling Yield of ^{68}Ga-NOTA-UBI-29-41 at Different Reaction Temperatures, for pH 3.5–4.0, 15–30 nmol of NOTA-UBI-29-41, and 23–38 MBq of ^{68}Ga

Temperature (°C)	% yield*
20	93.7 ± 5.7 ($n = 5$)
90	95.9 ± 4.4 ($n = 5$)

*Values represent average ± SD of $n = 5$.
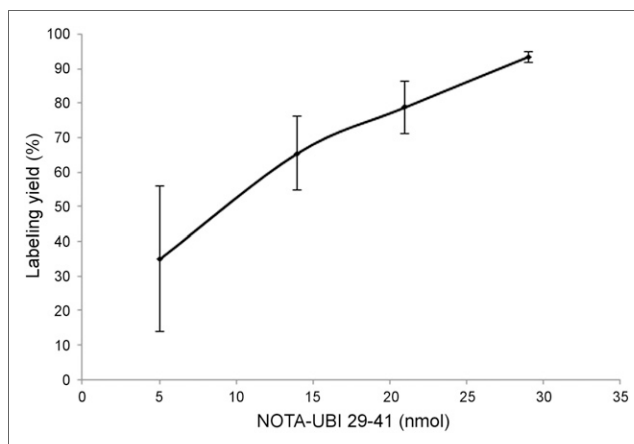
FIGURE 2. Labeling yield for increasing amounts of peptide for starting activity of 42 MBq of ^{68}Ga incubated at 20°C for 10 min (average ± SD; $n = 2$).

infection foci could be visualized on PET/CT (Fig. 6). The ^{68}Ga-NOTA-UBI-29-41 uptake was significantly higher in infected than in inflamed mice.

Confirmation of Infection. Culture of homogenized muscles confirmed the presence or absence of *S. aureus* (Fig. 7). *S. aureus* was not found in any of the contralateral muscles, nor was it detected in any of the muscles of inflamed mice. Culture of the excised infected muscle revealed the presence of viable *S. aureus*, correlating with the T/NT values. Even with levels of 2.5×10^4 cfu/g,

TABLE 2
Percentage of ^{68}Ga-NOTA-UBI-29-41 Bound to Plasma Proteins by Time

Time (min)	% bound to plasma proteins*
30	37.4 ± 0.2
60	44.1 ± 2.6
90	50.6 ± 2.6
120	51.7 ± 2.5

*Values are average ± SD of $n = 2$.

FIGURE 3. Percentage of ^{68}Ga-NOTA-UBI-29-41 bound to increasing amount of *S. aureus,* expressed as percentage of activity bound over total activity (% B/T) vs. colony-forming units ($n = 2$).

FIGURE 4. Biodistribution of ^{68}Ga-NOTA-UBI-29-41 expressed as percentage of activity (%IA) per gram for each organ or tissue in healthy mice ($n = 4$) at 30, 60, and 120 min after injection (A) and in healthy, inflamed, and infected mice ($n = 4$) at 60 min after injection (B).

the T/NT was 2.5 at 60 min after injection, whereas for inflammation, the T/NT at the same time was 1.6.

DISCUSSION

In this study, ^{68}Ga-NOTA-UBI-29-41 was labeled and characterized by HPLC, ITLC-SG, and SPE. High yield and radiochemical purity (>96%) were obtained with no need of further purification. The radiolabeled peptide was stable up to 3 h.
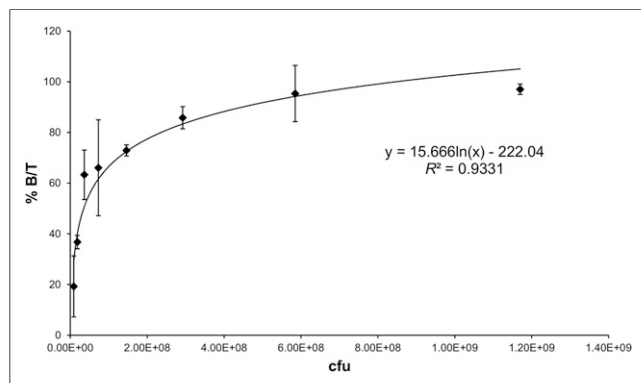
The analytic systems used to determine and quantify the different radiochemical impurities, including ^{68}Ga colloid, were successful and in concordance with previous studies (*16*).

^{68}Ga is obtained from a ^{68}Ge/^{68}Ga generator (*15, 17–19*), which facilitates the labeling of NOTA-UBI-29-41 for clinical use in sites having no cyclotron. Previously, we have used SPECT with ^{99m}Tc-UBI-29-41 in infected mice and rabbits (*4,5,20,21*). In this study, we have used ^{68}Ga-NOTA-UBI-29-41 to analyze its in vivo biology in infection, inflammation, and healthy mouse models and to evaluate its potential as a PET/CT tracer for the targeting of bacterial infection. Our aim is to transfer previous knowledge to this new positron-emitter radionuclide without compromising the infection imaging properties of UBI-29-41. The labeling of this peptide with ^{99m}Tc was done by a direct method of reduction with KBH$_4$ and SnCl$_2$ involving Arg and Lys residues (*22*). For the labeling with ^{68}Ga otherwise, a chelating agent attached to Thr is required. DOTA is the most commonly used chelating agent, but we selected NOTA because it has a smaller diameter, greater stability, faster labeling kinetics, and greater in vivo stability (*13*). The NOTA-UBI-29-41 was labeled using ^{68}Ga, which was eluted from an organic-based generator by fractionated elution, a simple but reliable method to increase concentration. Labeling was successful, and postpurification was not needed because of the high yields and the negligible amounts of colloid. Furthermore, we have confirmed that ^{68}Ga-NOTA-UBI-29-41 is stable in vitro for at least 3 h. Biodistribution data of ^{68}Ga-NOTA-UBI-29-41 in healthy mice at different times after injection revealed high urinary elimination, moderate uptake in the kidneys, and negligible uptake in the liver. This biologic pattern does not interfere with the image quality. Biodistribution studies indicated specific uptake in infected tissues as evidenced by the T/NT ratio of approximately 5 at 60 min after injection, maintaining values higher than 4.1 for up to 120 min. Studies in mice with ^{99m}Tc-UBI-29-41 revealed a similar pattern (*21*). This indicates that the conjugation with NOTA and the further labeling with ^{68}Ga do not alter the in vivo properties of UBI-29-41. Our study confirms values for percentage injected dose in liver, kidney, and bladder urine similar to those reported by Ebenhan et al. (*23*). All tissues except the kidneys showed a peak tracer concentration at 60 min that decreased slightly until 120 min. Our study also successfully determined the activity levels in blood and urine samples. We observed that 75% ± 14% of the injected activity was recovered in total urine 120 min after injection, which agrees with a previous study (*21*). Fifty-two percent of the ^{68}Ga-NOTA UBI-29-41 was bound to plasma proteins in 2 h, which also agrees with the percentage distribution to blood
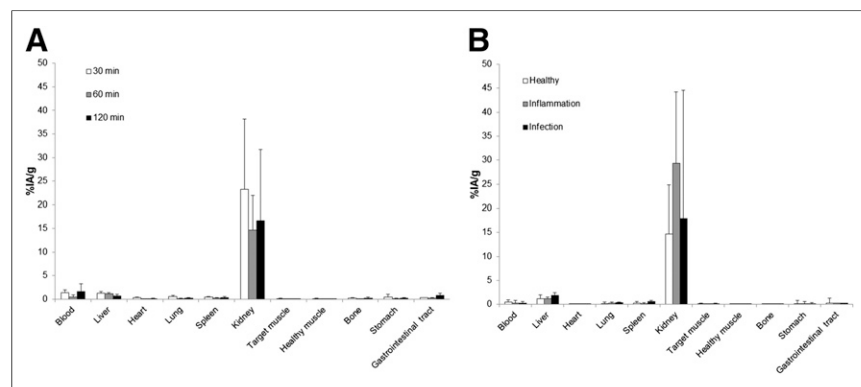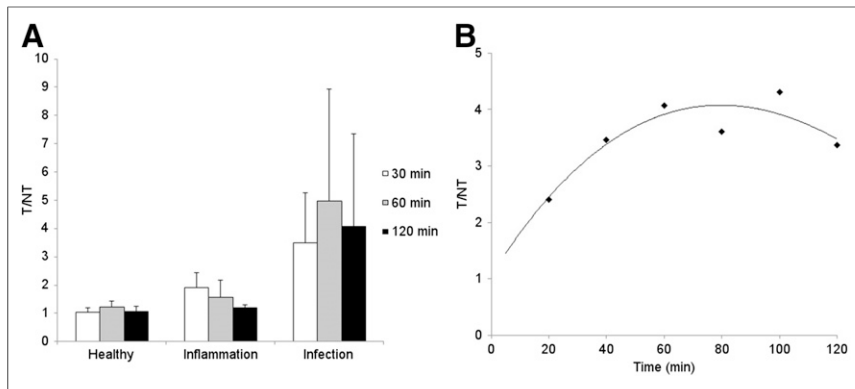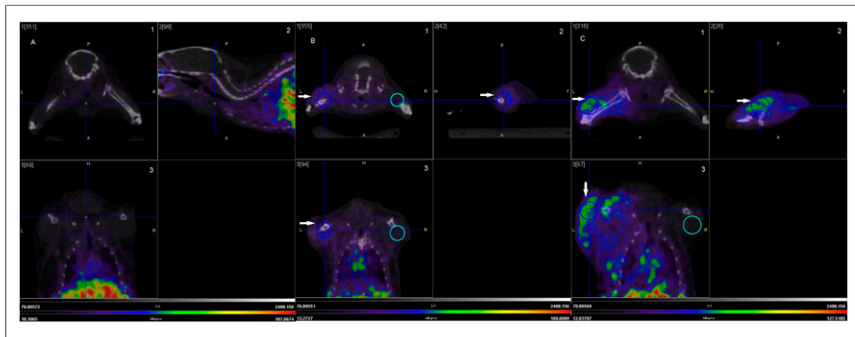
FIGURE 5. (A) T/NT for healthy, inflamed, and infected mice at 30, 60, and 120 min after injection, expressed as mean ± SD for at least 4 mice ($n = 1$ for B). (B) T/NT of infected mice calculated from volumes of interest of PET/CT images at different times after injection.

FIGURE 6. PET/CT images of healthy mouse (A), mouse with sterile inflammation (B), and mouse infected with *S. aureus* (C). Images were acquired 2 h after injection of ^{68}Ga-NOTA-UBI-29-41 (1, coronal; 2, sagittal; and 3, axial). Images correspond to frame 2 of 4. Arrows indicate inflamed or infected muscle.
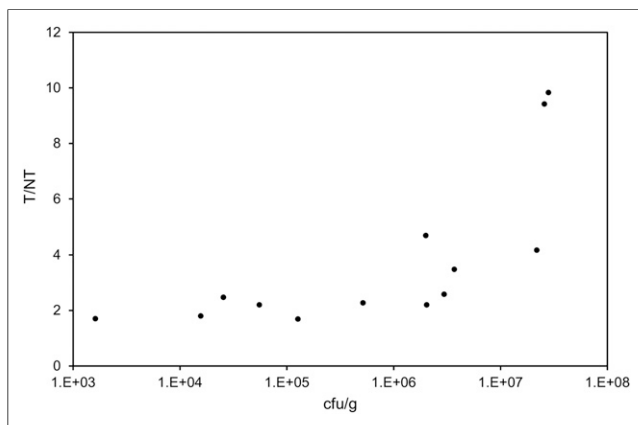
FIGURE 7. *S. aureus* recovered from infected muscle of mice ($n = 13$) after injection of ^{68}Ga-NOTA UBI-29-41 correlated with T/NT ratio, expressed as cfu/g. $y = 5 \times 10^{-7}x + 1.9562$ ($R^2 = 0.0982$) for x from 1×10^3 to 1×10^5 cfu/g; and $y = 2 \times 10^{-7}x + 2.5016$ ($R^2 = 0.7185$) for x from 1×10^5 to 1×10^8 cfu/g.

plasma fraction and blood cells (*21*). The two clinical studies performed with ^{99m}Tc-UBI-29-41 support our findings of gradual blood activity decline and similar accumulation in urine (*24,25*).

It has been suggested that antimicrobial peptides bind selectively to bacterial cytoplasmic membranes. The cationic peptide residues are capable of interacting electrostatically with the anionic regions of bacterial membranes (*14,26*). As described by Ferro-Flores et al. (*27*), UBI-29-41 fragment is a cationic human antimicrobial peptide with 6 positively charged residues (5 Arg + 1 Lys) and no cysteine. In the direct labeling with ^{99m}Tc, the amine groups of Lys and Arg 7 are presumably involved. Our labeling with ^{68}Ga was made incorporating the radionuclide into the NOTA core attached to Thr; thus, neither Arg nor Lys is likely involved. This method enhances the overall cationic charge of the peptide molecule, increasing the probability of electrostatic interactions with the bacterial wall. Experimentally, this finding was reflected by the almost 100% reached for the in vitro binding of ^{68}Ga-NOTA-UBI-29-41 to *S. aureus*.

Biodistribution and imaging studies were performed at 30, 60, and 120 min in mice bearing infection and sterile inflammation. The optimal time for T/NT ratio as well as for blood clearance was 60 min. ^{68}Ga-NOTA-UBI-29-41 uptake was greater in infected muscle than in healthy tissue in 18 of 18 mice, indicating high sensitivity. We inoculated 3 mice with *S. aureus* 48 h before the administration of ^{68}Ga-NOTA-UBI-29-41 to confirm the degree of infection suitable for detection. We found similar results to those for the mice inoculated 24 h before the administration of the tracer. The muscular infection in mice produced significantly greater accumulation than in inflamed and healthy mice at all the measured times (T/NT, $P \leq 0.002$). No significant differences ($P = 0.817$) were found among the groups of healthy and inflamed mice (ANOVA and Tukey statistical test). T/NT ratios calculated from PET/CT images for infected mice allowed differentiation between infection and inflammation from 10 min (T/NT > 2.4) and increased gradually to a maximum of 60 min (T/NT > 4.0), decreasing slightly up to 120 min (T/NT > 3.4) after injection.

Culture of the excised infected muscle revealed the presence of viable *S. aureus*, correlating with the T/NT values (Fig. 7). Even amounts of bacteria on the order of 10^4 were enough to discriminate infected from sterile inflamed or healthy mice 1 h after injection of ^{68}Ga-NOTA-UBI-29-41, which clearly indicates that the radiotracer discriminates bacterial infection from sterile inflammation.

The in vitro binding of ^{68}Ga-NOTA-UBI-29-41 to increasing amounts of *S. aureus* shows that the binding capacity of UBI-29-41 was maintained despite the conjugation of NOTA to the peptide and the labeling with ^{68}Ga. The maximum binding reached almost 100%, indicating the high specificity of the labeled molecule.

CONCLUSION

The labeling of ^{68}Ga-NOTA-UBI-29-41 was optimized at different temperatures, times, and pH conditions. The optimal ratio activity per peptide was determined, allowing a high specific activity. In vitro binding of ^{68}Ga-NOTA-UBI-29-41 to *S. aureus*

shows that the labeling does not alter the binding capacity, which reaches a maximum of approximately 100% and indicates high sensitivity. High uptake of ^{68}Ga-NOTA-UBI-29-41 was observed by PET/CT and biodistribution studies in infected tissues. All the infection foci were clearly delineated by the PET/CT acquisitions from 30 min after injection. A positive correlation was found between the number of colony-forming units recovered from infected tissues and the T/NT ratio. These facts revealed the high binding capacity of ^{68}Ga-UBI-29-41 to bacteria, both in vitro and in vivo. Compared with SPECT with ^{99m}Tc-UBI-29-41, PET/CT with ^{68}Ga-NOTA-UBI-29-41 represents an important improvement. The uptake, distribution, and excretion of UBI-29-41 were not significantly compromised by the conjugation with NOTA despite the differences in structure from ^{99m}Tc-UBI-29-41. Our findings demonstrate that ^{68}Ga-NOTA-UBI-29-41 can discriminate in vivo infection from inflammation, which means it has an excellent potential for clinical use. More research is necessary concerning the binding to other bacteria and fungi.

DISCLOSURE

ACKNOWLEDGMENTS

REFERENCES

1. Sathekge M. The potential role of ^{68}Ga-labelled peptides in PET imaging of infection. *Nucl Med Commun.* 2008;29:663–665.
2. Gemmel F, Dumarey N, Welling M. Future diagnostic agents. *Semin Nucl Med.* 2009;39:11–26.
3. Welling MM, Lupetti A, Balter HS, et al. ^{99m}Tc-labelled antimicrobial peptides for detection of bacterial and *Candida albicans* infections. *J Nucl Med.* 2001;42:788–794.
4. Welling MM, Paulusma-Annema A, Balter HS, Pauwels EK, Nibbering PH. Technetium-99m labelled antimicrobial peptides discriminate between bacterial infections and sterile inflammations. *Eur J Nucl Med.* 2000;27:292–301.
5. Nibbering PH, Welling MM, Paulusma-Annema A, Brouwer CP, Lupetti A, Pauwels EKJ. ^{99m}Tc-labelled UBI 29-41 peptide for monitoring the efficacy of antibacterial agents in mice infected with *Staphylococcus aureus. J Nucl Med.* 2004;45:321–326.
6. Brouwer CP, Bogaards SJ, Wulferink M, Velders MP, Welling MM. Synthetic peptides derived from human antimicrobial peptide ubiquicidin accumulate at sites of infections and eradicate (multi-drug resistant) *Staphylococcus aureus* in mice. *Peptides.* 2006;27:2585–2591.
7. Ferro-Flores G, Arteaga De Murphy C, Pedraza-López M, et al. In vitro and in vivo assessment of ^{99m}Tc-UBI specificity for bacteria. *Nucl Med Biol.* 2003;30:597–603.
8. Decristoforo C, Pickett RD, Verbruggen A. Feasibility and availability of ^{68}Ga-labelled peptides. *Eur J Nucl Med Mol Imaging.* 2012;39(suppl 1):S31–S40.
9. Morphy JR, Parker D, Alexander R, et al. Antibody labelling with functionalised cyclam macrocycles. *J Chem Soc Chem Commun.* 1988;3:156–158.
10. Craig AS, Parker D, Adams H, Bailey NA. Stability, [71]Ga NMR, and crystal structure of a neutral gallium(III) complex of 1,4,7-triazacyclononanetriacetate: a potential radiopharmaceutical? *J Chem Soc Chem Commun.* 1989;23:1793–1794.
11. Eisenwiener K-P, Prata MIM, Buschmann I, et al. NODAGATOC, a new chelator-coupled somatostatin analogue labeled with ([67/68]Ga) and (^{111}In) for SPECT, PET, and targeted therapeutic applications of somatostatin receptor (hsst2) expressing tumors. *Bioconjug Chem.* 2002;13:530–541.
12. Lewis MR, Raubitschek A, Shively JE. A facile, water-soluble method for modification of proteins with DOTA: use of elevated temperature and optimized pH to achieve high specific activity and high chelate stability in radiolabeled immunoconjugates. *Bioconjug Chem.* 1994;5:565–576.
13. Velikyan I. Synthesis, characterization and application of ^{68}Ga-labelled peptides and oligonucleotides [thesis]. Uppsala, Sweden: Uppsala University; 2004.
14. Lupetti A, Nibbering PH, Welling MM, Pauwels E. Radiopharmaceuticals: new antimicrobial agents. *Trends Biotechnol.* 2003;21:70–73.
15. Breeman WAP, de Jong M, de Blois E, Bernard BF, Konijnenberg M, Krenning EP. Radiolabelling DOTA-peptides with [68]Ga. *Eur J Nucl Med Mol Imaging.* 2005;32:478–485.
16. Ebenhan T, Chadwick N, Sathekge MM, et al. Peptide synthesis, characterization and ^{68}Ga-radiolabeling of NOTA-conjugated ubiquicidin fragments for prospective infection imaging with PET/CT. *Nucl Med Biol.* 2014;41:390–400.
17. Fani M, Andre J, Maecke H. ^{68}Ga-PET: a powerful generator-based alternative to cyclotron-based PET radiopharmaceuticals. *Contrast Media Mol Imaging.* 2008;3:67–77.
18. de Blois E, Sze Chan H, Naidoo C, Prince D, Krenning EP, Breeman WAP. Characteristics of SnO$_2$-based [68]Ge/^{68}Ga generator and aspects of radiolabelling DOTA-peptides. *Appl Radiat Isot.* 2011;69:308–315.
19. Chakravarty R, Chakraborty S, Dash A, Pillai MRA. Detailed evaluation on the effect of metal ion impurities on complexation of generator eluted ^{68}Ga with different bifunctional chelators. *Nucl Med Biol.* 2013;40:197–205.
20. Akhtar MS, Khan ME, Khan B, et al. An imaging analysis of ^{99m}Tc-UBI (29-41) uptake in *S. aureus* infected thighs of rabbits on ciprofloxacin treatment. *Eur J Nucl Med Mol Imaging.* 2008;35:1056–1064.
21. Welling MM, Mongera S, Lupetti A, et al. Radiochemical and biological characteristics of ^{99m}Tc-UBI 29-41 for imaging of bacterial infections. *Nucl Med Biol.* 2002;29:413–422.
22. Meléndez-Alafort L, Ramírez FDM, Ferro-Flores G, De Murphy CA, Pedraza-López M, Hnatowich DJ. Lys and Arg in UBI: a specific site for a stable Tc-99m complex? *Nucl Med Biol.* 2003;30:605–615.
23. Ebenhan T, Zeevaart JR, Venter JD, et al. Preclinical evaluation of ^{68}Ga-labeled 1,4,7-triazacyclononane-1,4,7-triacetic acid-ubiquicidin as a radioligand for PET infection imaging. *J Nucl Med.* 2014;55:308–314.
24. Meléndez-Alafort L, Rodríguez-Cortés J, Ferro-Flores G, et al. Biokinetics of ^{99m}Tc-UBI 29-41 in humans. *Nucl Med Biol.* 2004;31:373–379.
25. Akhtar MS, Qaisar A, Irfanullah J, et al. Antimicrobial peptide ^{99m}Tc-ubiquicidin 29-41 as human infection-imaging agent: clinical trial. *J Nucl Med.* 2005;46:567–573.
26. Yeaman MR, Yount NY. Mechanisms of antimicrobial peptide action and resistance. *Pharmacol Rev.* 2003;55:27–55.
27. Ferro-Flores G, Ramirez F, Melendez-Alafort L, Arteaga de Murphy C, Pedraza-Lopez M. Molecular recognition and stability of ^{99m}Tc-UBI 29-41 based on experimental and semiempirical results. *Appl Radiat Isot.* 2004;61:1261–1268.